

Practical formulation of accurate many-body potentials through the perturbative extension of diatomics-in-ionic-systems: Applied to HF clusters

M. Ovchinnikov and V. A. Apkarian^{a)}

Department of Chemistry, University of California, Irvine, California 92697-2025

(Received 21 December 1998; accepted 18 February 1999)

A perturbative extension of the diatomics-in-ionic-systems (DIIS) is formulated as a practical method for describing global many-body potential energy surfaces with accuracy and economy. The method is applied to HF clusters, generalizing the prior accurate DIIS treatment of the dimer [Grigorenko, Nemukhin, and Apkarian, *J. Chem. Phys.* **108**, 4413 (1998)] to arbitrary numbers of HF molecules. The calculated geometries, energetics, and harmonic frequencies of $(\text{HF})_n$, $n = 2-6$ clusters agree in detail with the available data on this well-studied system. The formulation is based on treating intermolecular interactions within perturbation theory. It is shown that second-order perturbation, which includes bimolecular excitations, is necessary and sufficient in describing the many-body potential energy surfaces with spectroscopic accuracy. The approach allows the analysis of H-bonding and its nonadditive induction and dispersion forces in terms of mixings and exchange between ground- and excited states of dimers including intra- and intermolecular charge-transfer states as well as molecular triplet states. The speed of evaluation of the potential scales is the cube of the number of molecules, providing a practical method for dynamical simulations of extended hydrogen-bonded networks. © 1999 American Institute of Physics. [S0021-9606(99)30119-7]

I. INTRODUCTION

The proper representation of many-body potential energy surfaces (PES) is perhaps the most fundamental challenge to molecular descriptions of chemical physics in condensed media. The desired attributes of such a representation are that it be simultaneously:

- Accurate*, the standard for which is set by spectroscopic measurements.
- Universal*, that a single set of parameters allow descriptions ranging from the pair to the bulk.
- Global*, that the derived PES be valid for all accessible configurations of the system.
- Economical*, that the formulation allow efficient evaluation of the PES for extended systems, to be useful in numerical simulations of structure and dynamics in condensed media on representative time and size scales.

In this paper we develop the perturbative extension of the diatomics-in-molecules (DIM) formulation as a general method that fulfills the above criteria. For the purposes of a nontrivial illustration, and as a rigorous test of the method, we consider the prototypical hydrogen bonded network of HF clusters. The challenges provided by this system, and the extant understanding which is based on extensive experimental and theoretical work has been recently summarized by Quack and Suhm.¹ Earlier, we had demonstrated that the diatomics-in-ionic-systems (DIIS) extension of DIM provided an accurate description of the PES of the HF dimer.² The direct implementation of that method to systems of ar-

bitrary size is impractical, because the basis sets required for the evaluation of the Hamiltonian matrices expand exponentially with the number of molecules. In the present work we show how to overcome this difficulty with *economy* while retaining attributes inherent to the DIIS approach, namely its *global nature* and the *accuracy* already demonstrated in the case of $(\text{HF})_2$. Further, by explicitly considering clusters up to hexamer, we provide a rigorous test for the proper accounting of nonadditivities of intermolecular interactions i.e., the *universality* of the formulated PES. The approach of using DIIS for the description of intermolecular interactions fundamentally differs from the more traditional treatments of force fields, or classical potentials expressed in terms of atom-atom functions and electrostatic interactions between distributed charges and polarizable centers. We highlight these fundamental differences as we outline the method and results.

II. THEORY

A. Overview

The formulation of the diatomics in molecules (DIM) method has been well documented.³⁻⁵ Succinctly, the treatment is based on the partition of the electronic Hamiltonian of a system into single-atom and diatomic contributions:

$$H_{\text{DIM}} = \sum_{a < b} H_{ab} - (N-2) \sum_a H_a. \quad (1)$$

The polyatomic basis functions are chosen to be antisymmetrized products of defined atomic states, leading to polyatomic basis functions that are direct products of atomic bases. The single atom Hamiltonians H_a are diagonal matri-

^{a)} Author to whom correspondence should be addressed.

ces of atomic energies and the diatomic contributions H_{ab} are constructed based on a chosen model of the diatomic $a-b$. Potential energy functions of the $a-b$ fragments, or their linear combinations, serve as input to H_{ab} .

Although the formulation is exact, its application as such is impractical since the exact expansion of molecular eigenstates into the product of atomic states requires very large atomic bases, and complete input for all states of all diatomic fragments is never known. The semiempirical implementations of DIM seek useful truncations of the required atomic bases, and therefore an appropriate partitioning of the diatomic Hamiltonian in this basis. In effect, it is assumed that in the chosen limited atomic basis the Hamiltonian matrix remains additive. This assumption cannot hold in systems containing strong polar bonds, where interactions are dominated by nonadditive electrostatic forces. The proper treatment of such systems within a strict DIM formalism would require the inclusion of a large number of Rydberg and ionized atomic states in the basis. The DIIS extension of the theory solves this problem by the addition of nonpairwise terms to the Hamiltonian (1) in the form of electrostatic interactions between charges and polarizable particles.⁶ It is useful to code this term in operator notation:

$$H = H_{\text{DIM}} - \sum_a \frac{1}{2} \hat{\alpha}_a \left(\sum_b \frac{\hat{q}_b \mathbf{r}_{ba}}{r_{ba}^3} \right)^2, \quad (2)$$

where $\hat{\alpha}_a$ is the polarizability and \hat{q}_a is the charge operator of the atom a . The operator notation of charge and polarizability in (2) highlights the fact that these assume different values for different atomic states and cannot in general be substituted by their average magnitudes. For example, the charge operator has eigenvalues $\pm 1e^-$ for ionic states of an atom and 0 for neutral states; \hat{q}_a can therefore be thought of as a projection operator which yields the ionicity in mixed polyatomic states. Beside induction, the DIIS term in Eq. (2) also includes dispersion through the polarizability operator and has significant differences from classical descriptions of electrostatic interactions between partial charges and polarizable molecules. This distinction is clarified in Appendix A, by considering the illustrative example of an HF molecule interacting with a polarizable particle (such as Ar). Classical treatments cannot reproduce the nonadditivity in electrostatic interactions contained in the description of Eq. (2).

Both DIM and DIIS have found widespread utility in describing the interactions of one or two open-shell atoms interacting with many closed-shell atoms, as in the case of radicals and excited states of molecules in rare gas hosts. An overview of this development has been given in a recent review article.⁷ This limited use of the method to describing intermolecular interactions can be traced to the fact that the inclusion of many rare-gas atoms does not expand the basis set beyond what is required for the description of the open shell fragments. The perturbative extension of the method developed here is designed to overcome this limitation, to enable the description of extended molecular systems of arbitrary electronic structure. It is therefore useful to consider the basis sets required for direct implementations, prior to proceeding with the perturbation treatment.

B. Basis set

In the previous work the DIIS Hamiltonian was constructed for the HF dimer, and was shown to give a spectroscopically accurate PES.² We use that as the starting point for the present development. The polyatomic basis functions (PBF) are generated from the following atomic states: Seven states for F atoms, which include six $^2P(\text{F})$ spin-orbital states of the neutral atom and one $^1S(\text{F}^-)$ state of the ion; three states for H atom, including two $^2S(\text{H})$ and one $^1S(\text{H}^+)$. This would lead to a total of $(3 \times 7)^n$ states in the basis set of $(\text{HF})_n$, e.g., 441 states for the dimer. The requirement of overall charge neutrality, and restriction of states to an overall spin multiplicity of singlet, leads to significant reduction in dimensionality, especially for small n . The actual number of states deemed necessary to calculate the dimer surface was 31. The procedure of truncating the basis set to the ‘‘important configurations’’ is by nature empirical. Even with the reduced basis of the dimer, the direct implementation of the method to larger systems is not practical because of the ‘‘exponential runaway’’ in dimensionality. We therefore resort to the perturbation theoretical approach, which is described in detail in subsec. D. In essence, we treat the intermolecular interactions as a perturbation to the intramolecular Hamiltonian, which we describe in the next section. Note that with the usual assumption of zero overlap,⁴ the constructed PBFs are taken to be orthogonal. Both charge and polarizability operators of (2) are diagonal in this basis. The diagonal element of charge for each state is simply its value. Further, we partition the Hamiltonian such that the atomic polarizabilities required in Eq. (2) are taken to be their respective atomic values for the neutral states and zero for the excited ionic states. This allows the writing of the polarizability operator as

$$\hat{\alpha}_A = \alpha_A (1 - \hat{q}_A). \quad (3)$$

C. Model of HF monomer

Within the chosen atomic basis set only two $^1\Sigma$ states of the HF molecule can be constructed. These are:

$$\begin{aligned} |n\rangle &= F(^2P_{z,1/2})H(^2S_{-1/2}) - F(^2P_{z,-1/2})H(^2S_{1/2}) \\ \text{and } |i\rangle &= F(^1S)H(^1S), \end{aligned} \quad (4)$$

where z is the molecular axis, and the number subscripts indicate the projection of atomic spin on an arbitrary axis. The $^1\Sigma$ ground state of the molecule is therefore a superposition of these pure neutral $|n\rangle$ and ionic $|i\rangle$ states. The coupling between these two states is given by the mixing parameter $\beta(r_{\text{HF}})$ which depends on bond length. The two $^1\Sigma$ eigenstates of the intramolecular Hamiltonian are therefore:

$$|g\rangle = \cos \beta |n\rangle - \sin \beta |i\rangle, \quad (5a)$$

$$|e\rangle = \sin \beta |n\rangle + \cos \beta |i\rangle. \quad (5b)$$

The functional forms of the mixing parameter $\beta(r)$ and the diatomic potentials of ground- and excited $^1\Sigma$ states are shown in Fig. 1. It should be evident from the figure that the bonding in HF is dominated by the mixing of ionic character

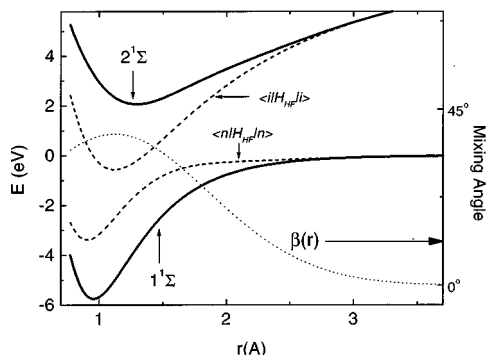


FIG. 1. The energies of 1Σ states in HF monomer in coupled (solid curves) and uncoupled (dashed curves) representations. The dotted line represents the mixing function $\beta(r)$. (A) The schematic diagram of the energy levels in the HF-Ar system.

in the neutral state, and this mixing assumes a value of 38% near the equilibrium bond length of the molecule. The model of the monomer is somewhat different from that used in the previous work. The description and the basis for the empirically adjusted parameters of these functions are given in Appendix B. Within the zero overlap description in monomers, i.e., $\langle i|n \rangle = 0$, the charges on each atom can be described by the projection operator

$$\hat{Q} = |i\rangle\langle i|. \quad (6)$$

The partial charges $+\delta$ on H and $-\delta$ on F in the ground electronic state are then given by

$$\delta = \langle g|\hat{Q}|g \rangle = \sin^2 \beta, \quad (7)$$

and the transition dipole moment between the two states can be evaluated using the relationship

$$\mu_{ge} = \langle g|\hat{Q}r_{HF}|e \rangle = \sin \beta \cos \beta r_{HF}. \quad (8)$$

The excited states of the monomer that can be obtained from this atomic basis are: $2^1\Sigma$ ($|e\rangle$ state), 1Π , 3Σ , 3Π , and the ionic states $2\Sigma(\text{HF}^-)$, $2\Sigma(\text{FH}^+)$, and $2\Pi(\text{FH}^+)$. All states except the $2^1\Sigma$, have distinct symmetries, and therefore uniquely correlate with the defined atomic states.

D. Perturbative DIIS

The Hamiltonian (2) can be divided into intra- and intermolecular contributions:

$$H = H_{\text{intra}} + H_{\text{inter}}. \quad (9)$$

The intramolecular part, unperturbed Hamiltonian, is the sum of monomer Hamiltonians

$$H_{\text{intra}} = \sum_{i=1}^n H_{H_i F_i}. \quad (10)$$

The intermolecular part is treated as a perturbation, which can be written as:

$$H_{\text{inter}} = \sum_{i=1}^n \sum_{j=i+1}^n \left(\sum_{A,B=H,F} H_{A_i B_j} \right) - \sum_{i=1}^n \sum_{j=1, j \neq i}^n \sum_{k=1, k \neq i}^n \left(\sum_{A,B,C=H,F} \frac{\hat{\alpha}_{A_i}}{2} \hat{q}_{B_j} \hat{q}_{C_k} \times \frac{(\mathbf{r}_{A_i B_j} \cdot \mathbf{r}_{A_i C_k})}{r_{A_i B_j}^3 r_{A_i C_k}^3} \right), \quad (11)$$

where the squares in the DIIS term of (2) have been explicitly multiplied out. The solution of the unperturbed Hamiltonian is direct: given the ground state of a single molecule $|g\rangle$, the system ground state is the product of the molecular ground states

$$|\Gamma\rangle = \prod_{i=1}^n |g_i\rangle. \quad (12)$$

E. First-order correction

The intermolecular interaction energy in first-order perturbation is:

$$V^{(1)} = \langle \Gamma | H_{\text{inter}} | \Gamma \rangle, \quad (13)$$

which is evaluated by substitution of (11) and (12) into (13) and by taking the expectation value of each term in the sum. The first summation over dimers i, j includes terms

$$\langle \Gamma | H_{A_i B_j} | \Gamma \rangle = \langle g_i, g_j | H_{A_i B_j} | g_i, g_j \rangle, \quad (14)$$

where A and B denote atoms (either H or F). This is a dimer problem which is evaluated by decomposing the molecular state into the defined atomic states using Eq. (5a), and applying the standard DIM procedure of rotating the fragment Hamiltonians from the fragment fixed frame (both in coordinate and spin space) into the frame fixed on molecules i and j . For the matrix elements that involve neutral states the spin state of the fragment $A_i B_j$ is defined by the singlet states of molecules i and j which are defined superpositions of singlet and triplet states, namely, the singlet and triplet diatomic potentials enter the fragment Hamiltonian with 1/4 and 3/4 coefficients, respectively. It should be noted that this term of the many-body Hamiltonian is pairwise additive, i.e., the overall energy is the sum of dimer interaction energies. Explicit expressions, along with the forms of the rotation and spin-coupling matrices have already been given.²

The first-order expression in the electrostatic part of the Hamiltonian (11) includes three-body terms. The summation is over three molecules $i, j \neq i, k \neq i$. When $j=k$ the contribution is from two-body interactions. These terms in $V^{(1)}$ have the form

$$- \frac{(\mathbf{r}_{A_i B_j} \cdot \mathbf{r}_{A_i C_k})}{r_{A_i B_j}^3 r_{A_i C_k}^3} \left\langle g_i, g_j, g_k \left| \frac{\hat{\alpha}_{A_i}}{2} \hat{q}_{B_j} \hat{q}_{C_k} \right| g_i, g_j, g_k \right\rangle. \quad (15)$$

To evaluate this expression, we note that since no intermolecular charge transfer is included, the charge and polarizability operators can be replaced by the state projection operator (6):

$$\hat{q}_{H_i} = -\hat{q}_{F_i} = \hat{Q}_i \quad \text{and} \quad \hat{\alpha}_{A_i} = \alpha_A(\hat{I} - \hat{Q}_i), \quad (16)$$

where \hat{I} is the unit operator. After this substitution, expression (15) is evaluated using the relationships (6–8). The important difference from the classical electrostatic interaction comes from the fact that \hat{Q} is a projection operator and $\hat{Q}^2 = \hat{Q}$ (see Appendix A).

F. Second-order correction

Even though the first-order correction is not pairwise-additive, it is still a sum of two- and three-body contributions. The true nonadditivity comes from mixing with the excited states of the system, i.e., through the second-order correction in the perturbation expansion which results in a new wavefunction of the system

$$|\Psi\rangle = |\Gamma\rangle + \sum_{\chi} \frac{\langle \Lambda^{\chi} | H_{\text{inter}} | \Gamma \rangle}{E_{\chi}} |\Lambda^{\chi}\rangle, \quad (17)$$

where the index χ enumerates all excited states of the system Λ^{χ} . As is shown in the results section, the first-order term recovers 84% of the binding energy in the dimer, however, the shape of the potential surface is significantly modified by the second-order correction. In larger clusters the first-order

energy is a poorer approximation. For example, in $(\text{HF})_6$, the first-order term recovers only 45% of the binding energy at the minimum geometry. In principle, the number of all excited state configurations is the dimensionality of the basis. However, the number of important excitations is significantly smaller. We may classify the excitations of the system by the number of molecules involved, by writing the second-order contribution to the energy as an expansion

$$V^{(2)} = \sum_{i=1}^n \sum_{\xi} \frac{\langle \Gamma | H_{\text{inter}} | \Lambda_i^{\xi} \rangle \langle \Lambda_i^{\xi} | H_{\text{inter}} | \Gamma \rangle}{E_{\xi}} + \sum_{i=1}^n \sum_{j=i+1}^n \sum_{\kappa} \frac{\langle \Gamma | H_{\text{inter}} | \Lambda_{ij}^{\kappa} \rangle \langle \Lambda_{ij}^{\kappa} | H_{\text{inter}} | \Gamma \rangle}{E_{\kappa}} + \dots \quad (18)$$

The first term involves the summation over excited states Λ_i^{ξ} by which we denote the excitation of a single molecule i to a monomer excited state ξ . The second term represents pair excitations Λ_{ij}^{κ} of the ij pair into the excited state κ , with restrictions of charge neutrality and spin conservation.

For the monomer term the allowed excitations are $\xi = 2^1\Sigma(|e\rangle), {}^1\Pi_x, {}^1\Pi_y$. The coupling elements are obtained by explicit substitution of Hamiltonian (11) as follows:

$$\begin{aligned} \langle \Gamma | H_{\text{inter}} | \Lambda_i^{2^1\Sigma} \rangle &= \sum_{j=1, j \neq i}^n \left(\sum_{A, B = \text{H, F}} \langle g_i, g_j | H_{A_i B_j} | e_i, g_j \rangle \right) \\ &\quad - \sum_{j=1, j \neq i}^n \sum_{k=1, k \neq i}^n \left(\sum_{A, B, C = \text{H, F}} \left\langle g_i, g_j, g_k \left| \frac{\alpha_{A_i}}{2} q_{B_j} q_{C_k} \frac{(\mathbf{r}_{A_i B_j} \cdot \mathbf{r}_{A_i C_k})}{r_{A_i B_j}^3 r_{A_i C_k}^3} \right| e_i, g_j, g_k \right\rangle \right) \\ &\quad - 2 \sum_{j=1, j \neq i}^n \sum_{k=1, k \neq j}^n \left(\sum_{A, B, C = \text{H, F}} \left\langle g_i, g_j, g_k \left| \frac{\alpha_{A_j}}{2} q_{B_i} q_{C_k} \frac{(\mathbf{r}_{A_j B_i} \cdot \mathbf{r}_{A_j C_k})}{r_{A_j B_i}^3 r_{A_j C_k}^3} \right| e_i, g_j, g_k \right\rangle \right), \end{aligned} \quad (19)$$

$$\langle \Gamma | H_{\text{inter}} | \Lambda_i^{2^1\Pi} \rangle = \sum_{j=1, j \neq i}^n \left(\sum_{B = \text{H, F}} \langle g_i, g_j | H_{F_i B_j} | ({}^1\Pi)_i, g_j \rangle \right). \quad (20)$$

Note that the order of summations is reduced by 1 from expression (11), since elements of the sum that do not include the excited molecule i result in zero due to the orthogonality of PBFs.

The pair excitations, beside simultaneous excitation of two monomers, include intermolecular charge-transfer configurations and molecular triplet states coupled into an overall singlet. Thus, the summation in (18) is over: (i) simultaneous excitations of monomers: $\kappa = (2^1\Sigma, 2^1\Sigma), (2^1\Sigma, {}^1\Pi), ({}^1\Pi, {}^1\Pi)$; (ii) triplet states: $\kappa = ({}^3\Sigma, {}^3\Sigma), ({}^3\Sigma, {}^3\Pi), ({}^3\Pi, {}^3\Pi)$; (iii) intermolecular charge-transfer states: $\kappa = ({}^2\Sigma(\text{HF}^-), {}^2\Sigma(\text{FH}^+)), ({}^2\Sigma(\text{HF}^-), {}^2\Pi(\text{FH}^+))$. Coupling to these excitations, including all the spatial components, are obtained by explicit algebraic evaluations similar to those in Eqs. (19) and (20). It is useful to consider expressions for some of the important configurations, to recognize the mechanisms of coupling.

The only pair excitation for which the electrostatic part is important is $\kappa = (2^1\Sigma, 2^1\Sigma)$:

$$\begin{aligned} \langle \Gamma | H_{\text{inter}} | \Lambda_{ij}^{(2^1\Sigma, 2^1\Sigma)} \rangle &= \sum_{A, B = \text{H, F}} \langle g_i, g_j | H_{A_i B_j} | e_i, e_j \rangle \\ &\quad - \sum_{k=1, k \neq i}^n \left(\sum_{A, B, C = \text{H, F}} \left\langle g_i, g_j, g_k \left| \frac{\alpha_{A_i}}{2} q_{B_j} q_{C_k} \frac{(\mathbf{r}_{A_i B_j} \cdot \mathbf{r}_{A_i C_k})}{r_{A_i B_j}^3 r_{A_i C_k}^3} \right| e_i, e_j, g_k \right\rangle \right) \\ &\quad - \sum_{k=1, k \neq i, j}^n \left(\sum_{A, B, C = \text{H, F}} \left\langle g_i, g_j, g_k \left| \frac{\alpha_{A_j}}{2} q_{B_i} q_{C_k} \frac{(\mathbf{r}_{A_j B_i} \cdot \mathbf{r}_{A_j C_k})}{r_{A_j B_i}^3 r_{A_j C_k}^3} \right| e_i, e_j, g_k \right\rangle \right). \end{aligned} \quad (21)$$

The triplet excited states are coupled through the neutral component of the ground-states as

$$\begin{aligned} \langle \Gamma | H_{\text{inter}} | \Lambda_{ij}^{(3\Sigma, 3\Sigma)} \rangle &= \sum_{A,B=H,F} \langle g_i, g_j | H_{A,B} | {}^3\Sigma_i, {}^3\Sigma_j \rangle \\ &= \cos \beta(r_i) \cos \beta(r_j) \sum_{A,B=H,F} \langle n_i, n_j \\ &\quad \times | H_{A,B} | {}^3\Sigma_i, {}^3\Sigma_j \rangle. \end{aligned} \quad (22)$$

The latter matrix element is evaluated using spin rotation of the fragment Hamiltonian. The most important contribution of the coupling among triplets comes from $H_i F_j$ interactions, which leads to the admixture of singlet-state pair potentials into the interaction between H-bonded H and F, and therefore the strengthening of the H-bond.

The intermolecular charge-transfer states contribute via terms

$$\begin{aligned} \langle \Gamma | H_{\text{inter}} | \Lambda_{ij}^{(2\Sigma(\text{HF}^-), 2\Sigma(\text{HF}^+))} \rangle &= \sum_{A,B=H,F} \langle g_i, g_j | H_{A,B} | {}^2\Sigma(\text{HF}^-)_i, {}^2\Sigma(\text{HF}^+)_j \rangle \\ &= \cos \beta(r_i) \sin \beta(r_j) \\ &\quad \times \langle P_z(\text{F}_i), S(\text{F}_j^-) | H_{\text{F}_i, \text{F}_j} | S(\text{F}_i^-, P_z(\text{F}_j)) \rangle \\ &\quad - \sin \beta(r_i) \cos \beta(r_j) \\ &\quad \times \langle S(\text{H}_i), S(\text{H}_j^+) | H_{\text{H}_i, \text{H}_j} | S(\text{H}_i^+, S(\text{H}_j)) \rangle \\ &\quad + \langle g_i, g_j | H_{\text{H}_i \text{F}_j} | {}^2\Sigma(\text{HF}^-)_i, {}^2\Sigma(\text{HF}^+)_j \rangle, \end{aligned} \quad (23)$$

in which there are two distinct mechanisms of coupling: (i) the first two terms couple ionic-neutral configurations through the exchange interaction in H_2^+ and F_2^- fragments; (ii) the last term is the mixing by the intermolecular $H_i F_j$ Hamiltonian which is contained in the coupling of neutral and ionic ${}^1\Sigma$ states, as described in subsection C.

III. NUMERICAL IMPLEMENTATION

Based on the above formalism we have developed a C++ package for the calculation of the ground state PES with an arbitrary number of HF molecules. The main routine uses the number of molecules n and coordinates as input, and outputs the first-order correction to the energy $V^{(1)}$ and the arrays of couplings between the ground-state and all single- and double-molecular excitations $C_i^{(\xi)}$ and C_{ij}^{κ} , respectively. This allows us to obtain the energy of the system at the second-order approximation in perturbation theory and allows an analysis of the wavefunction. The structure of the program resembles that of Eq. (11). It consists of two parts. The first performs a double cycle over all molecules, treats the first part of the Hamiltonian, and scales as n^2 . The second part, which treats the electrostatic contributions, scales as n^3 . The calculation of the coupling elements increases the length of calculations by only a few times as compared to the calculation of the first-order correction and does not change the scaling of the program. The DIM matrix computations (part of the program that scales as n^2) are the most expensive

for the sizes of the clusters considered in this paper. It is not clear at present at which system size the n^3 scaling takes effect. At present, we have not included analytical derivatives of the PES in the package.

IV. RESULTS AND DISCUSSION

A. Dimer

The PES obtained by the perturbative DIIS to second-order agrees with the full DIIS treatment to within 1 cm^{-1} throughout. Based on the second-order correction to energy, $C^2/E \sim 100 \text{ cm}^{-1}$ for the largest contributions which correspond to the ionic-neutral interactions and therefore $E \sim 10 \text{ eV}$ (see Table I), it is then possible to estimate the next order correction in perturbation as

$$V^{(3)} \approx \frac{C^3}{E^2} \approx 1 \text{ cm}^{-1}. \quad (24)$$

Although the dimer surface has been discussed in detail elsewhere,^{1,2} it is useful to dissect it into first- and second-order contributions, to make conclusions about the additivity of the various terms in the potential. As in other works on the dimer we analyze the surface by fixing the F–F distance and consider potential energy contours as a function of the in-plane rotation angles θ_1, θ_2 . The first-order energy $V^{(1)}$, its various terms, and comparison with the full PES is shown in Fig. 2. The first-order surface is very similar to that of the full treatment as far as the stable geometries of the dimer are involved. Thus, the general structure of the H-bond can be discussed within the first-order correction, i.e., by considering the fixed electronic structure on each molecule. The peculiar geometry of the dimer is the result of cancellation between anisotropic core and neutral-ionic interactions. For the sake of analysis, the first-order term may be decomposed into contributions from neutrals, ion-neutral, and ion–ion interactions:

$$\begin{aligned} \langle g, g | \hat{H}_{\text{inter}} | g, g \rangle &= \cos^4 \beta \langle n, n | \hat{H}_{\text{inter}} | n, n \rangle \\ &\quad + \cos^3 \beta \sin \beta \langle n, n | \hat{H}_{\text{inter}} | n, i \rangle + \dots \\ &\quad + \sin^4 \beta \langle i, i | \hat{H}_{\text{inter}} | i, i \rangle, \end{aligned} \quad (25)$$

of these, the ion-neutral term

$$V_{\text{H}^+\text{F}} = \cos^2 \beta \sin^2 \beta (\langle n, i | \hat{H}_{\text{H}_2 \text{F}_1} | n, i \rangle + \langle i, n | \hat{H}_{\text{H}_1 \text{F}_2} | i, n \rangle), \quad (26)$$

which simply describes the donor H^+ interacting with the F atom on the acceptor HF, imposes the L-shaped geometry as shown in Fig. 2(A), where a deep (-1430 cm^{-1}) minimum occurs at $\theta_1 = 0^\circ$, $\theta_2 = 90^\circ$. This is simply due to the fact that the Π potential of FH^+ is significantly more attractive than the Σ , reflecting the reduced electron density on the F atom along the Σ interaction and the preference of H^+ to point at the maximal electron density [see illustrated sidepanel in Fig. 2(A)]. The ionic interactions, given by the term

$$V_{\text{ionic}} = \sin^4 \beta \langle i, i | \hat{H}_{\text{inter}} | i, i \rangle, \quad (27)$$

TABLE I. The contribution of excited states to the wavefunction of the dimer at various geometries as given by Eq. (17).

Geometry:	$\theta_1 = -14.5^\circ, \theta_2 = 64.5^\circ$ minimum		$\theta_1 = 0^\circ, \theta_2 = 0^\circ$ saddle		$\theta_1 = -62^\circ, \theta_2 = 118^\circ$ saddle	
Excitation	$\frac{C^{(\Lambda)}}{E_\Lambda}$ ^a	$\frac{ C^{(\Lambda)} ^2}{E_\Lambda}$	$\frac{C^{(\Lambda)}}{E_\Lambda}$	$\frac{ C^{(\Lambda)} ^2}{E_\Lambda}$	$\frac{C^{(\Lambda)}}{E_\Lambda}$	$\frac{ C^{(\Lambda)} ^2}{E_\Lambda}$
$\Lambda =$ (Donor, Acceptor)		(cm^{-1})		(cm^{-1})		(cm^{-1})
Ionic states:						
(2 $^1\Sigma, 1^1\Sigma$)	0.038	161	0.024	64	0.021	46
(1 $^1\Sigma, 2^1\Sigma$)	0.020	48	0.032	112	0.021	46
(2 $^1\Sigma, 2^1\Sigma$)	-0.006	9	-0.013	39	-0.003	3
$^1\Pi$ states:						
(1 $^1\Sigma, 1^1\Pi_x$)	0	0	0	0	0	0
($1^1\Pi_x, 1^1\Sigma$)	0	0	0	0	0	0
($1^1\Pi_x, 1^1\Pi_x$)	0	0	0	0	0	0
($1^1\Pi_y, 1^1\Pi_y$)	0	0	0	0	0	0
Triplet states:						
($3^3\Sigma, 3^3\Sigma$)	0	0	0.013	47	0.003	3
($3^3\Sigma, 3^3\Pi_x$)	0.007	11	0	0	0	0
($3^3\Pi_x, 3^3\Sigma_u$)	0	0	0	0	0	0
($3^3\Pi_x, 3^3\Pi_x$)	0	0	0	0	0	0
($3^3\Pi_y, 3^3\Pi_y$)	0	0	0	0	0	0
charge transfer states:						
($2^2\Sigma(F^-H), 2^2\Sigma(FH^+)$)	0.006	5	0.013	26	0.006	6
($2^2\Sigma(F^-H), 2^2\Pi_x(FH^+)$)	0.003	1	0	0	0.004	3
($2^2\Sigma(FH^+), 2^2\Sigma(F^-H)$)	0.011	18	0.003	2	0.006	6
($2^2\Pi_x(FH^+), 2^2\Sigma(F^-H)$)	0.004	2	0	0	0.004	3
$V^{(1)}, V^{(2)}$ (cm^{-1})	1338, 252		876, 281		1117, 107	
Induced dipole moments of the molecules (D)						
$\delta\mu_D, \delta\mu_A$	0.11, 0.058		0.070, 0.093		0.061, 0.061	

^a $C^{(\Lambda)} = \langle \Lambda | H_{\text{inter}} | \Gamma \rangle$ are the coupling elements of the excited states Λ to the ground state. Only the states of $^1A'$ symmetries (with respect to the $z-x$ plane of the dimer) are included in the table. An entry 0 in the table means that the coefficients are less than 10^{-3} and energy contributions are less than 0.5 cm^{-1} .

which include the combination of Coulomb, induction, and dispersion forces calculated through DIIS lead to a deeper minimum (-2360 cm^{-1}) at the linear geometry $\theta_1 = \theta_2 = 0^\circ$ as shown in Fig. 2(B). The competition of these forces leads to the geometry of $(\text{HF})_2$. The complete first-order surface, $V^{(1)}$, that includes all the terms of expression (25) is shown in Fig. 2(C). The minima of the surface nearly coincide with the minima of the full treatment, up to second-order, shown in Fig. 2(D).

The most significant difference that results in the second-order correction occurs at the saddle point at $(0^\circ, 0^\circ)$ geometry of the dimer. This is where mixing with the excited states of the molecules plays the most significant role. In Table I we give a complete analysis of the wavefunction in terms of mixing coefficients with all excited states of the molecules as given by Eq. (17) and list the contributions of each excitation to the energy. We consider three geometries of the dimer: $(-15^\circ, 64^\circ)$ —the minimum of the surface; $(0^\circ, 0^\circ)$ —linear saddle point; and $(-62^\circ, 118^\circ)$ —saddle point along the H-bond switching coordinate. We also include the total first-order, $V^{(1)}$, and second-order $V^{(2)}$ contributions to the potential and the induced dipole moments of the molecules in these geometries in the table.

Ionic excitations, which describe the bond polarization represent the most significant nonadditive forces. Ionic excitation of the donor is the most important contribution at the minimum geometry of the complex, contributing $\sim 10\%$ of the binding (161 cm^{-1}) in this geometry and leads to the induced dipole moment of the donor molecule $\delta\mu_D = 0.11 \text{ D}$ in addition to the intrinsic dipole of the HF monomer $\mu_0 = 1.7965 \text{ D}$.⁸ Ionic excitation of the acceptor has a comparable effect on the linear geometry of the dimer (112 cm^{-1}) and leads to $\delta\mu_A = 0.093 \text{ D}$ induced dipole moment. While the coupling to the simultaneous ionic excitation of donor and acceptor is an order-of-magnitude smaller than the single excitations, it has a significant variation with geometry and its inclusion is important for obtaining the proper surface. Note, as would be expected, this contribution preferentially stabilizes the linear geometry, where it lowers the energy by 39 cm^{-1} .

There is negligible mixing between the ground-state and singlet-excited-neutral states.

Among the triplet excitations, which necessarily involve double excitations, the largest is the contribution of $(^3\Sigma, ^3\Sigma)$ state of the dimer described by the matrix element of Eq. (20). This term describes the covalent contribution to the

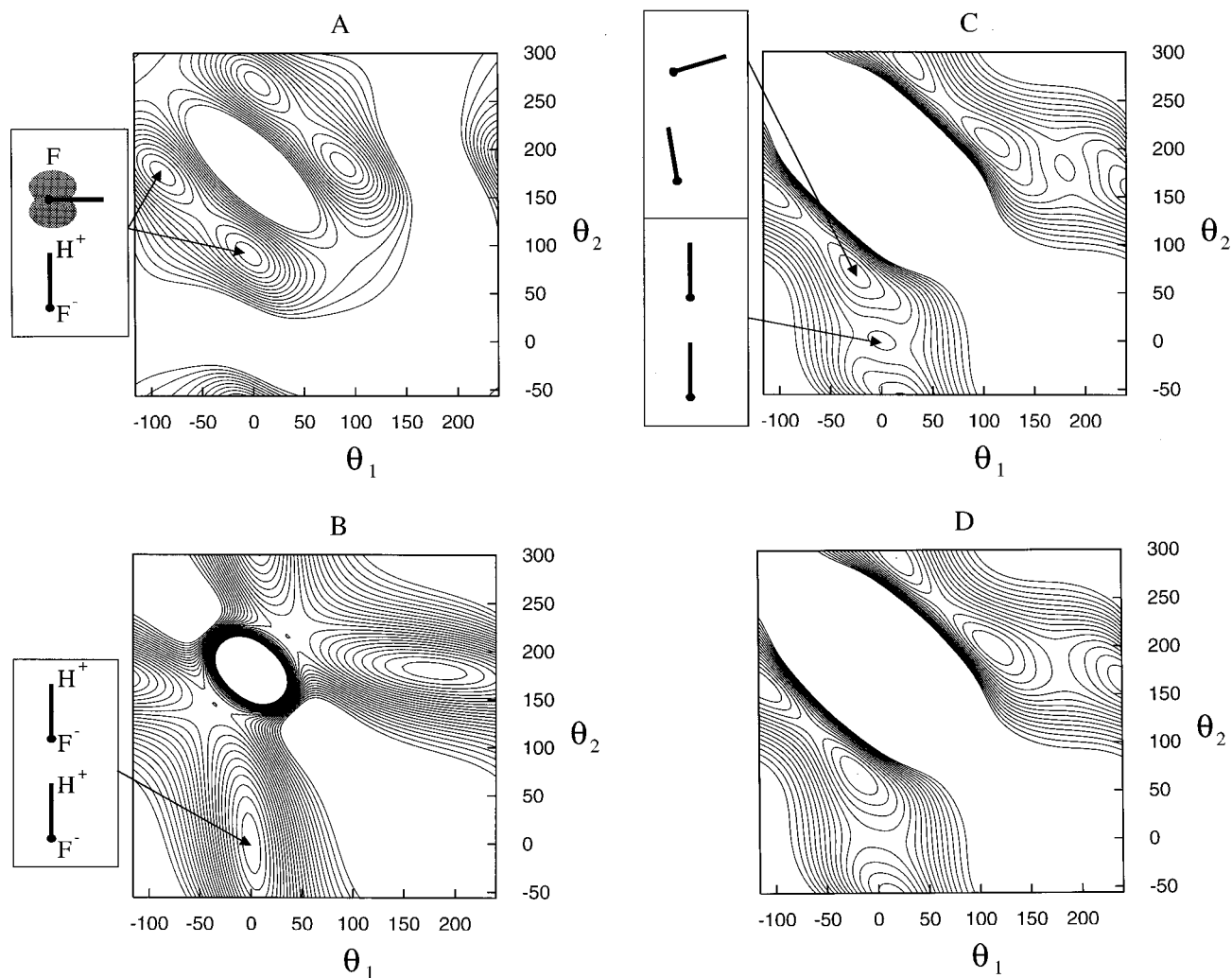


FIG. 2. Various contributions to the $(\text{HF})_2$ PES. (A) Contribution of the H^+F interactions responsible for L-shaped geometry of the dimer. (B) Contribution of the ionic interactions. (C) The first order PES of the dimer, $\langle \Gamma | H_{\text{inter}} | \Gamma \rangle$. (D) Full PES calculated in the second-order of the perturbation theory. θ_1 and θ_2 are the angles of in-plane rotation of H atoms around F atoms. The F–F distance is 2.75 Å. The contours are separated by 100 cm^{-1} and are not shown above zero.

hydrogen bond. It becomes important at small HF distances and is largest for the linear geometry. The mechanism of this coupling can be well understood. The $1^1\Sigma$ is the deep attractive ground-state potential of HF molecule. However, in first-order perturbation, the intermolecular HF interaction is described by the linear combination of singlet and triplet states

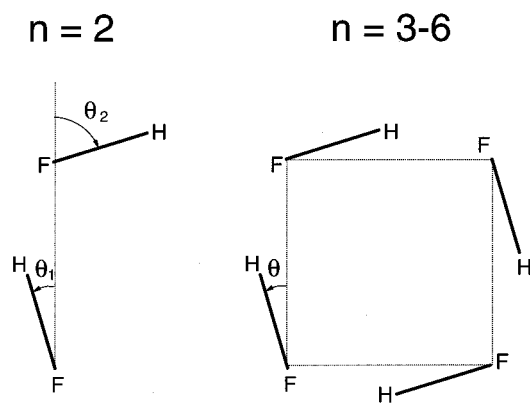
$$V_{\Sigma} = \frac{1}{4} V_{1\Sigma} + \frac{3}{4} V_{3\Sigma}, \quad (28)$$

where the ratio is fixed because of the fixed-spin ground-states of the molecules. Mixing with triplets relaxes this constraint and allows to increase the contribution of singlet character, thus allowing for greater attraction between H and F.

Intermolecular charge transfer states have two mechanisms of coupling according to Eq. (23). The exchange interaction in the HH^+ and FF^- fragments is a mechanism similar to that of the mixing among triplets. This contribution, in effect, increases the covalency of the bond since the charge transfer is symmetric, i.e., the expectation values of

charge on the donor and acceptor molecules remain unchanged. The mechanism that leads to the actual transfer of the charge is the Hamiltonian of HF that is not diagonal in the neutral-ionic basis. The values of the charge transferred from one molecule to the other are small, but geometry dependent. At the equilibrium geometry, the net electron transfer is from donor to acceptor, with a charge asymmetry of $\sim 4 \times 10^{-5}$, while in the linear geometry the net electron transfer is from acceptor to donor, with a net charge asymmetry of $\sim 1 \times 10^{-4}$. While the contributions to the energetics of the system is relatively small, $\sim 25 \text{ cm}^{-1}$, they are required to reproduce these sections of the PES to within their known accuracy. The net dipole of the dimer in our model yields a value of 2.78 D, this is to be compared with the experimental value of 2.988 D,⁹ while the most recent *ab initio* calculations yield 3.333 D.¹⁰

The subtle interplay of polarization and exchange interactions, which are analyzed here as the admixture of various excited state configurations in the ground-state wavefunction, determine the dimer PES which seems well reproduced.

FIG. 3. The geometries of $(\text{HF})_n$ clusters.

B. $(\text{HF})_n$, $n=3-6$

The minimum energy structures of the clusters are found by Monte Carlo simulated annealing. Various initial geometries are used to ensure that the determined minima are global. In all cases the stable structures are cyclic, as in the case of the tetramer illustrated in Fig. 3. The calculated binding energies and geometric parameters of the clusters are collected in Table II, along with the recommended values by Quack and Suhm.¹ In addition, we list the induced dipole moment of the molecules in the clusters which are based on our analysis of the wavefunctions. The harmonic vibrational frequencies of the clusters, which are obtained by diagonalization of the numerically computed mass-weighted Hessian, are collected in Table III. These are compared with the harmonic frequencies obtained from surfaces which yield good agreement with experiments when corrected for anharmonicities, where such comparisons have been possible.¹ In the case of dimer and trimer we also include the results from most recent *ab initio* calculations.¹⁰ It should be pointed out that, while the reference dimer PES to which we compare our results has been rigorously tested and adjusted to reproduce experiments, the parameters of the larger clusters are less well established. The spectroscopic data on the clusters is sparse and not well resolved; quantum calculations of structure are less reliable, and exact quantum treatments of dynamics are not possible yet. Despite these precautionary comments, the HF clusters remain among the best character-

ized systems, and the trends in structure and energetics as a function of cluster size are quite reliable. Finally, in Table IV we list the contributions of the various excitations to the ground-state wavefunction and energy at the equilibrium geometry of each cluster.

The comparison in Table II shows that the calculated binding energies, H-F bond length, and F-F distances are reproduced to within the known accuracy of these parameters for all clusters. The comparison is somewhat poorer in the case of the bond angles, being consistently larger in our treatment than the reference values. The exact origin of this systematic discrepancy is not clear. It can be attributed to either the quality of the input parameters, namely the chosen functional form of potentials and mixing parameter in the DIIS treatment. The input parameters can in principle be refined to yield a better agreement, however, we have refrained from making arbitrary adjustments, even though the accuracy of the potentials used at the internuclear H-F distances (1.6–1.8 Å) is questionable.

With regard to the vibrational frequencies of the clusters, the available data are rather sparse. We report all predicted frequencies, and this should help in the experimental identification of modes that have not yet been studied. Where comparisons are possible, it appears that the predicted frequencies are in line with the known values, except for the out-of-plane librations which are systematically ~25% lower than the reference values. This discrepancy is directly related to that of the bond angles. The effective masses of normal modes associated with these librations include moments of inertia for rotation of H atoms around the F-F axes. If these masses are proportional to the squares of bond angles, a linear decrease in the out-of-plane librational frequency with the opening of the H-F-F angle would be expected.

Based on all other comparisons, e.g., the extension of the HF bond length and the associated contraction of the intermolecular F-F bond length with cluster size, it is clear that the nonadditive interactions of the hydrogen bonding network is rather accurately reproduced in this treatment. This gives confidence in other structural and dynamical predictions. For example, the hydrogen bond strength (D_e/n for $n>2$, D_e for dimer) is linearly correlated with the H-F stretching frequency, consistent with the Badger correlation.¹¹ Also, it is interesting to note that the ring puck-

TABLE II. Geometries, energies, and induced dipole moments of $(\text{HF})_n$, $n=2-6$ clusters.

n	Binding energy D_e (cm^{-1})		Bond lengths r_{HF} (Å)		Distance between nearest F atoms. R_{FF} (Å)		Angles θ_{HFF}		Induced dipole moment $\delta\mu$ (D)
	This work	Ref. 1	This work	Ref. 1	This work	Ref. 1	This work	Ref. 1	This work
	2	-1595	-1590	0.921	0.920	2.76	2.735	14.5°	7°
			0.923	0.923			64.5°	68°	0.058
3	-5287	-5266	0.932	0.933	2.58	2.59	31.6°	24°	0.188
4	-9778	-9781	0.941	0.944	2.49	2.51	19.2°	12°	0.285
5	-13 270	-13 459	0.946	0.948	2.47	2.48	10.5°	6°	0.32
6	-16 043	-16 630	0.947	0.949	2.47	2.47	5.1°	3°	0.33

TABLE III. The contribution of the important excited states to the wavefunction of $(\text{HF})_n$, $n=3-6$ clusters at the minimum energy geometry.^a

n : Excitation κ	3		4		5		6	
	$\frac{C^{(\beta)}}{E_\beta}$	$\frac{ C^{(\beta)} ^2}{E_\beta}$ (cm^{-1})	$\frac{C^{(\beta)}}{E_\beta}$	$\frac{ C^{(\beta)} ^2}{E_\beta}$ (cm^{-1})	$\frac{C^{(\beta)}}{E_\beta}$	$\frac{ C^{(\beta)} ^2}{E_\beta}$ (cm^{-1})	$\frac{C^{(\beta)}}{E_\beta}$	$\frac{ C^{(\beta)} ^2}{E_\beta}$ (cm^{-1})
Ionic excitations ($2^1\Sigma$)	0.065	459	0.098	1042	0.112	1365	0.114	1430
Double ionic excitations ($2^1\Sigma, 2^1\Sigma$)	0.006	7	0.007	13	0.009	16	0.009	17
Triplet excitations of nearest neighbors	0.008	8	0.012	31	0.016	51	0.020	60
Donor-acceptor charge transfer	0.015	31	0.023	52	0.025	56	0.024	48
Acceptor-donor charge transfer	0.008	7	0.008	6	0.006	4	0.006	3

^aThe energies in the second column are given per single excitation. To obtain the total energy of the cluster the entries must be multiplied by the number of molecules, n .

ering modes (designated as F-F bend in Table IV) progressively soften with cluster size, reaching a value of $\sim 1 \text{ cm}^{-1}$ in the hexamer. Rather than the exact magnitude of this mode, its very low value should be taken as a reliable indicator that the out-of-plane distortion of the hexamer is very floppy. Given the large amplitudes associated with H atoms, the mean structure of the hexamer can be expected to be the boat conformation, a structure that has previously been reported in at least one study.¹² It is easy to predict that the heptamer is no longer planar, with nonplanarity imposed for optimization of intermolecular angles. Further, given the glo-

bal nature of the generated PES it is possible to consider larger amplitude dynamics, such as fragmentation or evaporation with some confidence. More relevant to the present is the inspection of the various competing terms that lead to the overall energetics of the clusters.

Inspection of Table IV shows that the second-order contributions to the overall energy of the cluster becomes increasingly more important as the size of the cluster increases. Thus, of the overall binding energy of the hexamer, $16\,043 \text{ cm}^{-1}$, $\sim 53\%$ is due to the second-order term arising from single ionic excitations of monomer units ($6 \times 1430 \text{ cm}^{-1}$).

TABLE IV. Harmonic frequencies ω_i of the $(\text{HF})_n$ clusters (cm^{-1}).^a

n	2			3			4		5		6	
	This work	Ref. 1	Ref. 10	This work	Ref. 1	Ref. 10	This work	Ref. 1	This work	Ref. 1	This work	Ref. 1
In plane librations	223 489,	210, 550	221, 583	586(2), 1001	600	616(2), 992	577 789(2), 1048	850	605(2), 861(2), 1045	950	529, 649(2), 873(2), 1009	700- 1000
Out of plane librations	322	465	491	361(2), 581	700	512(2), 713	409 499(2), 632	800	465(2), 543(2), 626	800	446 491(2), 544(2) 598	
F-F bend ^b							41, 96		18(2), 78(2)		1(3), 53(2), 111	
F-F stretch	125	155	166	163(2), 183	200	203(2), 226	177, 237(3)	280	149, 237(2), 302(2)	270	127 210(2), 309(2), 335	250
ω_{HF}	4024, 4079	4030, 4100	4039, 4112	3843, 3938(2)	3890	3761, 3880(2)	3649, 3818(2), 3890	3670	3528, 3728(2), 3848(2)	3640	3505 3694(2), 3822(2), 3871	3580

^aIn parentheses we list the degeneracies of the modes.

^bThese represent the in-plane and out-of-plane distortions of the skeletal structure, e.g., in the case of the tetramer the two frequencies are for the butterfly motion and rhombic distortion.

This dominant term represents the many-body polarization of the HF bond by as much as 18% in the hexamer. The contributions from other electronic configurations are significantly smaller, and more geometry specific. For example, the next most important term in the case of the hexamer is due to the singlet–triplet mixing which leads to an incremental $\sim 2\%$ stabilization of the cluster ($6 \times 60 \text{ cm}^{-1}$). The geometry dependence of various contributions (or equivalently, the optimal structure that results from the interplay of the various mixings) can be discerned by noting that in the trimer and tetramer the intermolecular charge transfer from donor to acceptor is the configuration that plays the more important role. Although the interplay between these couplings is rather subtle, with respect to the topologies of the PES, these contributions are quite significant. Quite clearly hydrogen bonding in these clusters is dominated by nonadditive interactions that cannot be hoped to be retrieved from classical potentials. Yet, with a single set of input parameters the DIIS approach retrieves the delicate balance of forces.

Finally, given the large second-order correction to total energy of oligomers, the convergence of the perturbation series becomes suspect. It is possible to estimate the next-order correction to total energy. To this end, we note that the second- and higher-order corrections are due to excited states containing ionic configurations, while the first-order energy is the result of cancellation between electrostatic stabilization (ion-neutral) and repulsion from the covalent core. The first-order stabilization energy of the hexamer due to the ionic configuration alone can be extracted directly as $\sim 50\,000 \text{ cm}^{-1}$, and it is this contribution that should be compared to the second-order correction of $\sim 8000 \text{ cm}^{-1}$. Based on a simple linear chain model for electrostatic interactions, we can estimate an overall contribution for $V(3) \sim 500 \text{ cm}^{-1}$. Thus the cluster size dependent discrepancy between our values for total binding energy and the reference data collected in Table II can be entirely attributed to limiting the perturbation treatment to second-order.

V. CONCLUSIONS

We have presented the perturbative extension of the diatomics-in-ionic-systems formulation as a practical method for describing many-body potentials with accuracy. The formulation was applied to the description of HF clusters, where interactions are known to be dominated by nonadditivities. With a single set of pair parameters as input, second order perturbation expansion of the DIIS Hamiltonian describes this well-studied prototype of hydrogen bonding with accuracy. Beside the efficiency in the evaluation of the global surfaces through strictly algebraic equations, the method provides a convenient means for dissecting the subtle interplay between forces involved in hydrogen bonding, as already discussed above. Given the general principles involved in the formulation, we would expect it to be broadly applicable where accurate treatments of extended molecular systems is required.

ACKNOWLEDGMENTS

This work has tremendously benefitted from interactions with Dr. B. L. Grigorenko and Professor A. V. Nemukhin. We thank both of them for the thorough discussions. We would also like to thank Dr. Grigorenko for making her codes available to us. This research was made possible through support from the NSF, under Grant No. CHE-9708382, and the US AFOSR, under Grant No. F49620-95-1-0213.

APPENDIX A: INTERACTION OF HF WITH POLARIZABLE PARTICLE

To illustrate the difference between the DIIS Hamiltonian (2) and classical parametrizations of intermolecular interactions, we consider the model example of a dipolar molecule interacting with a polarizable atom, as in the case of HF–Ar. Consider the long-range interaction and assume that the contribution of H_{DIM} is zero. Classically, the energy is due to the Coulombic interactions between the partial charges on the polar HF molecule and the polarizable particle

$$V_{cl} = -\frac{\alpha^2 \mathbf{E}}{2} = -\frac{\alpha^2 \mathbf{G}}{2} \delta^2, \quad (\text{A1})$$

where \mathbf{E} is the electric field due to the partial charges on H and F and we have defined the geometric factor \mathbf{G} as

$$\mathbf{G} = \frac{r_{\text{Ar-H}}}{r_{\text{Ar-H}}} - \frac{r_{\text{Ar-F}}}{r_{\text{Ar-F}}^3}. \quad (\text{A2})$$

whereas, the DIIS interaction is given as

$$H_{\text{int}} = -\frac{\alpha \mathbf{G}^2}{2} \hat{Q}^2. \quad (\text{A3})$$

In the $|n\rangle - |i\rangle$ basis the 2×2 matrix H_{int} has only one non-zero element:

$$\langle i | H_{\text{int}} | i \rangle = -\frac{\alpha \mathbf{G}^2}{2} \quad (\text{A4})$$

If the splitting between the ground- and excited states of HF $|g\rangle$ and $|e\rangle$ is large we can use the perturbation result

$$V_{\text{DIIS}} = \langle i | H_{\text{int}} | i \rangle = -\frac{\alpha \mathbf{G}^2}{2} \sin^2 \beta = -\frac{\alpha \mathbf{G}^2}{2} \delta. \quad (\text{A5})$$

Although the forms in (A1) and (A4) are the same, the classical solution is proportional to the square of partial charge, while the quantum result is linear in the partial charge on the atoms. This can lead to orders-of-magnitude difference in applications such as the one considered in the body of the text. Which is the correct result?

The proper answer to this question requires a more complete quantum treatment, taking into consideration that atomic polarization results from second-order coupling to excited states of the atom via the transition dipole. Representing the excited-state manifold on Ar by the single state $|1\rangle$ and denoting the ground-state as $|0\rangle$ (see illustration in Fig. 4), the polarizability of the atom is given as

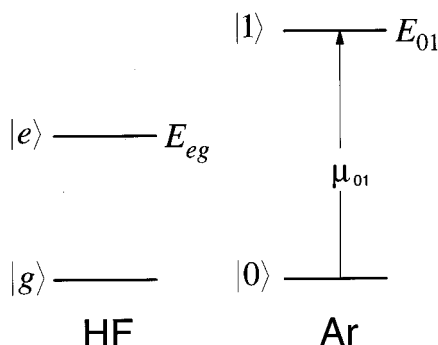


FIG. 4. The schematic diagram of the energy levels in the HF-Ar system.

$$\alpha = \frac{2\mu_{10}^2}{E_{10}}. \quad (\text{A6})$$

It is a reasonable approximation to take the energy E_{10} to be the ionization limit of Ar. The interaction Hamiltonian then couples the $|1\rangle$ and $|0\rangle$ states of Ar via the electrostatic interaction of transition dipole with charges. The second-order perturbation expression gives the result for the interaction energy

$$V = -\frac{|\langle g,0|\hat{\mu}\mathbf{G}\hat{Q}|g,1\rangle|^2}{E_{10}} - \frac{|\langle g,0|\hat{\mu}\mathbf{G}\hat{Q}|e,1\rangle|^2}{E_{10}+E_{eg}} \\ = -\mu_{01}^2\mathbf{G}^2\left(\frac{\sin^4\beta}{E_{10}} + \frac{\cos^2\beta\sin^2\beta}{E_{10}+E_{eg}}\right). \quad (\text{A7})$$

This full expression has two limits $E_{ge}\gg E_{01}$ and $E_{ge}\ll E_{01}$. In the first limit we neglect the second term in the sum, the first term simply gives us the classical answer. In the second limit we neglect the E_{ge} in the denominator of the second term and recover the quantum result. This solution gives the right physical picture: if the energy splitting of HF molecule is large, Ar sees it as a fixed partial charge, i.e., the excited state of HF does not enter the treatment. If the energy is small compared to the polarization energy of Ar, E_{01} , the polarizability can be replaced by an operator and the DIIS treatment must be used. In reality, the energies are comparable, with E_{01} greater by about a factor of 2 (10.2 eV compared to 15–20 eV ionization energies of atoms in the molecule) making the DIIS model more appropriate. While this suggests more exact decompositions of induction and dispersion terms, we take the more empirical approach in this work of accepting the utility of the DIIS model of Eq. (2), since it was shown to reproduce the PES for the dimer with spectroscopic accuracy.

APPENDIX B: MIXING OF 1Σ STATES IN HF MONOMER

The HF monomer ground-state, $|g\rangle$, used in this work is represented as an admixture between a neutral state, $|n\rangle$ and

ionic state, $|i\rangle$ with the mixing function $\beta(r)$ as given in the text by Eq. (5). The procedure for obtaining this decomposition is described here.

We start with the well characterized ground-state of the molecule described by the potential function $V_g = \langle g|H_{\text{HF}}|g\rangle$ as a given.² We assume the ionic state $V_i = \langle i|H_{\text{HF}}|i\rangle$ to be characterized by the sum of charge—charge and charge—induced dipole terms at long range, and by the exponentially screened Coulomb repulsion at short range:

$$V_i = -\frac{14.396}{r} - \frac{5.45}{r^4} + \frac{280.0}{r}e^{-3.6r} \quad (\text{eV}\cdot\text{\AA}), \quad (\text{B1})$$

in which the parameters for the repulsive wall are adjusted empirically to reproduce the dimer PES with the assumed form of the mixing function.

The mixing function, $\beta(r)$, was formerly estimated from an *ab initio* analysis to be a Gaussian.² We assume the same functional form but with a shift of the Gaussian center:

$$\sin^2\beta(r) = 0.512e^{-1.48(r-1.2)^2}. \quad (\text{B2})$$

The shift is necessary to simultaneously ensure the proper dipole at the equilibrium geometry of the monomer and a proper binding energy of the dimer. The increase of mixing parameter with molecular bond length at the equilibrium geometry is mainly responsible for the dependence of the bond length on the number of molecules in the H-bonded network. The function was accordingly adjusted to reproduce the HF bond lengths in the $n=2-4$ clusters. This is the extent of empiricism used in the present treatment. All other potential parameters are the same as those previously reported in the treatment of the dimer PES.²

¹M. Quack and M. A. Suhm, in *Conceptual Perspectives in Quantum Chemistry*, edited by J. L. K. Calais (Kluwer Academic, The Netherlands, 1997), pp. 415–463.

²B. L. Grigorenko, V. A. Nemukhin, and V. A. Apkarian, *J. Chem. Phys.* **108**, 4413 (1998).

³F. O. Ellison, *J. Am. Chem. Soc.* **85**, 3540 (1963).

⁴J. C. Tully, *Semiempirical Methods of Electronic Structure Calculation* (Plenum, New York, 1977).

⁵P. J. Kuntz, in *Atom-Molecule Collision Theory—A Guide for the Experimentalist*, edited by R. B. Bernstein (Plenum, New York, 1979).

⁶I. Last and T. F. George, *J. Chem. Phys.* **87**, 1183 (1987).

⁷V. A. Apkarian and N. Schwentner, *Chem. Rev.* **99** (to be published).

⁸K. P. Huber and G. Herzberg, *Molecular Spectra and Molecular Structure* (Van Nostrand Reinhold, New York, 1979).

⁹B. J. Howard, T. R. Dyke, and W. Klemperer, *J. Chem. Phys.* **81**, 5417 (1984).

¹⁰G. S. Tschumper, Y. Yamaguchi, and H. F. Schaefer, III, *J. Chem. Phys.* **106**, 9627 (1997).

¹¹R. M. Badger and S. H. Bauer, *J. Chem. Phys.* **5**, 839 (1937).

¹²H. Sun, R. O. Watts, and U. Buck, *J. Chem. Phys.* **96**, 1810 (1992).